HHS Public Access

Author manuscript

*Acta Biomater*. Author manuscript; available in PMC 2019 June 03.

Published in final edited form as:

*Acta Biomater*. 2017 September 01; 59: 21–32. doi:10.1016/j.actbio.2017.06.028.

# Enhanced In Vivo Retention of Low Dose BMP-2 Via Heparin Microparticle Delivery Does Not Accelerate Bone Healing in a Critically Sized Femoral Defect

**Marian H. Hettiaratchi**[1], **Tel Rouse**[2,3], **Catherine Chou**[1], **Laxminarayanan Krishnan**[3], **Hazel Y. Stevens**[6], **Mon-Tzu A. Li**[1], **Todd C. McDevitt**[4,5], and **Robert E. Guldberg**[3,6,*]

[1]The Wallace H. Coulter Department of Biomedical Engineering, Georgia Institute of Technology & Emory University, Atlanta, GA

[2]School of Chemical and Biomolecular Engineering, Georgia Institute of Technology, Atlanta, GA

[3]The Parker H. Petit Institute for Bioengineering and Bioscience, Georgia Institute of Technology, Atlanta, GA

[4]The Gladstone Institute of Cardiovascular Disease, San Francisco, CA

[5]The Department of Bioengineering and Therapeutic Sciences, University of California San Francisco, San Francisco, CA

[6]The George W. Woodruff School of Mechanical Engineering, Georgia Institute of Technology, Atlanta, GA.

## Abstract

Bone morphogenetic protein-2 (BMP-2) is an osteoinductive growth factor used clinically to induce bone regeneration and fusion. Some complications associated with BMP-2 treatment have been attributed to rapid release of BMP-2 from conventional collagen scaffolds, motivating the development of tunable sustained-release strategies. We incorporated BMP-2-binding heparin microparticles (HMPs) into a hydrogel scaffold to improve spatiotemporal control of BMP-2 delivery to large bone defects. HMPs pre-loaded with BMP-2 were mixed into alginate hydrogels and compared to hydrogels containing BMP-2 alone. BMP-2 release from scaffolds *in vitro*, BMP-2 retention within injury sites *in vivo*, and bone regeneration in a critically sized femoral defect were evaluated. Compared to hydrogel delivery alone, BMP-2-loaded HMPs reduced BMP-2 release *in vitro* and increased early BMP-2 retention in the bone defect. BMP-2-loaded HMPs induced bone formation at both ectopic and orthotopic sites; however, the volume of induced bone was lower for defects treated with BMP-2-loaded HMPs compared to hydrogel delivery. To better understand the effect of HMPs on BMP-2 release kinetics, a computational model was developed to predict BMP-2 release from constructs *in vivo*. The model suggested that HMPs limited BMP-2 release into surrounding tissues, and that changing the HMP density could modulate BMP-2 release. Taken together, these experimental and computational results suggest the importance of achieving a balance of BMP-2 retention within the bone defect and BMP-2 release

*Corresponding Author: Robert E. Guldberg, 315 Ferst Drive, Georgia Institute of Technology, Atlanta, GA 30332-0363 USA, robert.guldberg@me.gatech.edu.

into surrounding soft tissues. HMP delivery of BMP-2 may provide a method of tuning BMP-2 release *in vivo* that can be further investigated to improve current methods of bone regeneration.

## 1. Introduction

Large bone tissue defects resulting from traumatic injuries, tumor resections, and congenital defects are a particularly challenging problem for orthopedic surgeons, since they can often lead to inadequate healing and fracture non-union. This may occur as a result of the complex injury environment and a lack of robust biological cues to initiate and resolve the bone healing cascade [1–3]. The discovery and pharmaceutical production of bone morphogenetic proteins (BMPs) with osteogenic potential, particularly BMP-2 and BMP-7, have resulted in promising strategies to stimulate endogenous healing and bone growth [4–6]. BMP-2 has been delivered clinically using a collagen sponge scaffold, which, despite its absorbability and capacity for cell infiltration, cannot adequately retain BMP-2 within bone defect sites over long periods of time, in some cases demonstrating retention of <5% of the initial BMP-2 dose after 2 weeks *in vivo* [7–9]. The rapid release of BMP-2 from the collagen sponge and the use of high BMP-2 doses, have also been associated with numerous side effects in patients undergoing treatment for large bone defects, including excessive soft tissue inflammation and the formation of abnormal heterotopic bone [10–14].

Advanced biomaterials that can exert spatiotemporal control of BMP-2 presentation may improve clinical outcomes and reduce side effects associated with rapid BMP-2 release; several groups have developed biomaterials to improve BMP-2 delivery [15–17]. In our laboratory, we have developed a BMP-2 delivery system consisting of a degradable RGD-functionalized alginate hydrogel injected into the lumen of a polycaprolactone (PCL) nanofiber mesh tube [18–21]. This BMP-2 delivery vehicle can induce robust bone healing in a critically sized, rat femoral defect and restore the mechanical properties of the regenerated femurs to ~75% of intact bone [19]. Furthermore, when compared to BMP-2 delivery using the collagen sponge, the alginate construct prolonged BMP-2 retention and increased regenerated bone volume [18]. Despite these promising results, the persistence of BMP-2 within the bone defect remains relatively short, with >40% of the BMP-2 leaving the thigh within the first 3 days after administration [18, 21]. Since regeneration of damaged bone tissue is a dynamic process involving several weeks of coordinated cellular and biomolecular responses [22], the ability to maintain a substantial depot of bioactive BMP-2 within the bone defect over longer periods of time may improve the healing response.

Biomaterials containing affinity molecules, which strongly and/or specifically bind BMP-2 through non-covalent interactions, can increase BMP-2 retention *in vivo*. These include naturally occurring biomolecules with diverse growth factor binding abilities, such as heparin and fibronectin, or synthetic peptides and aptamers specifically engineered for unique growth factor binding [23]. Since heparin can electrostatically bind numerous growth factors in a reversible manner, a number of commonly used biomaterials have been “heparinized” to increase their growth factor loading capacity [24, 25]. Several studies have demonstrated that incorporating heparin chains into collagen sponges, calcium phosphate scaffolds, and various hydrogels can improve BMP-2 retention both *in vitro* and *in vivo* [26–

31]. In a previous study, we documented the fabrication of novel heparin methacrylamide microparticles (HMPs) possessing the ability to bind and retain large amounts of bioactive BMP-2. Loaded HMPs exhibited low BMP-2 release over 28 days *in vitro* (<10%) while maintaining the ability to induce robust cellular responses in C2C12 skeletal myoblasts [32]. These HMPs can be easily mixed into the hydrogel phase of alginate constructs, providing a simple method of incorporating a desired amount of heparin and subsequently increasing the growth factor loading capacity of the delivery system in a dose-dependent manner.

We investigated the incorporation and delivery of HMPs within alginate constructs to test two main hypotheses. Firstly, that loading BMP-2 onto HMPs would increase BMP-2 retention *in vivo* compared to delivery of soluble BMP-2 in alginate alone, and secondly, that this increased BMP-2 retention would subsequently increase bone formation *in vivo*. Subcutaneous implantation of biomaterials facilitated longitudinal tracking of fluorescently labeled BMP-2 [33], overcoming the limitation in fluorescent signal visualization observed in deeper tissues [34]. The femoral defect model provided a challenging test bed for bone healing, requiring the regeneration of functional, load-bearing bone [35]. Finally, to bridge the gap between *in vitro* and *in vivo* experimental results, a computational model was developed to gain understanding of the most relevant physical parameters determining the release and spatial distribution of BMP-2.

## 2. Materials and Methods

### 2.1. Fabrication of Heparin Microparticles

HMPs were fabricated as previously described [32] and as schematized in Figure 1A. Briefly, 55.6 mg of heparin methacrylamide, 18 mM ammonium persulfate (APS; Sigma Aldrich), and 18 mM tetramethylethylenediamine (TEMED; Sigma Aldrich) were dissolved in phosphate buffered saline (PBS; Corning Mediatech, Manassas, VA). 500 μL of heparin solution was homogenized for 5 minutes at 3000 rpm into a mixture of 60 mL of corn oil (Mazola) and 1 mL of polysorbate 20 (Promega, Madison, WI) using a Polytron PT3100 homogenizer (Kinematica, Lucerne, Switzerland). The emulsion was immersed in a 55°C water bath, and the free radical cross-linking reaction proceeded under constant stirring and nitrogen purging for 30 minutes. The solution was centrifuged for 10 minutes at 3000 rpm, and the resulting HMP pellet was washed once in acetone and several times in dd$H_2O$, prior to being disinfected in 70% ethanol for 30 minutes. The HMPs were lyophilized (Labconco, Kansas City, MO) and stored at 4°C until use.

### 2.2. Alkaline Phosphatase Activity

BMP-2 bioactivity was evaluated by culturing skeletal myoblasts (C2C12; ATCC, Manassas, VA) with soluble BMP-2 and BMP-2-loaded HMPs, and measuring the alkaline phosphatase (ALP) activity response [32]. 0.1 mg of HMPs were incubated with 35 ng of BMP-2 (Pfizer Inc. New York, NY) in 1 mL of 0.1% (w/v) bovine serum albumin (BSA) in PBS for 16 hours at 4°C under gentle rotation to achieve BMP-2 loading of 30 ng per 0.1 mg of HMPs. Unloaded HMPs, which were incubated in 1 mL of 0.1% BSA in PBS, and 30 ng of soluble BMP-2 treatment served as controls. To investigate the ability of HMPs to maintain BMP-2 bioactivity over longer periods of time, BMP-2-loaded HMPs, unloaded HMPs, and soluble

BMP-2 were also incubated at 37°C under gentle rotation for 2 weeks prior to evaluation of ALP induction.

ALP activity assays were performed as previously described [32]. C2C12 cells were seeded at a density of 62,500 cells/cm$^2$ on tissue culture polystyrene plates (Corning Inc., Corning, NY) for 6 hours in growth media (16% fetal bovine serum (FBS; Thermo Scientific Hyclone, Logan, UT) in DMEM (Corning Mediatech, Manassas, VA). Following cell attachment, the media was exchanged to low serum media (1% FBS in DMEM) containing treatments (HMPs and soluble BMP-2). Cells were cultured for an additional 72 hours before lysing with CelLytic M (Sigma Aldrich). Cell lysate was incubated with p-nitrophenyl phosphate substrate (Sigma Aldrich) to determine ALP activity or incubated with a fluorescent dsDNA-binding dye to determine DNA content (Quantifluor dsDNA Kit, Promega). Images were taken of cells incubated with HMPs stained with 1,9-dimethylmethylene blue (DMMB; Sigma Aldrich) on a Nikon Eclipse TE2000-U inverted microscope (Nikon Instruments, Melville, NY) to demonstrate relative cell and HMP density.

### 2.3. Fabrication of Alginate Constructs

Tissue engineered constructs were fabricated as previously described [19], and consisted of an alginate hydrogel contained within a polycaprolactone (PCL) nanofiber mesh tube. Irradiated, RGD-functionalized alginate (FMC Biopolymer, Philadelphia, PA) was slowly dissolved in equal volumes of α-MEM (Corning Mediatech, Manassas, VA) and 0.1% rat serum albumin (RSA; Sigma, Aldrich) in 4 mM HCl to obtain a 2% (w/v) alginate solution. The requisite amounts of BMP-2 (0–5 μg) and/or HMPs (0–1 mg) per 150 μL of alginate were added to the solution in 0.1% RSA in HCl. The alginate solution was cross-linked with excess calcium sulfate (8.4 mg/mL; Sigma Aldrich) by rapid mixing, and was equilibrated at room temperature for 30 minutes before being transferred to 4°C for storage overnight.

PCL nanofiber mesh tubes were fabricated as previously described [19]. Briefly, PCL (Sigma Aldrich) was dissolved in 90:10 hexafluoro-2-propanol (Sigma Aldrich) and dimethylformamide (Sigma Aldrich) at 12% (w/v) and electrospun onto aluminum foil, creating a mesh with an approximate thickness of 500 μm. Perforated rectangular sheets (12 mm by 19 mm with 23 0.9-mm diameter holes) cut from meshes were rolled into tubes having an inner diameter of 4.5 mm and length of 12 mm and glued using UV cure adhesive (DYMAX, Torrington, CT). Mesh tubes were sterilized by immersion in ethanol overnight, and stored in α-MEM up until use.

150 μL of alginate were injected through a blunt-tip needle into the center of each mesh tube. For *in vitro* assays, alginate was allowed to set in the tube for at least 10 minutes prior to immersion in any solution. For *in vivo* studies, alginate was injected into the tube immediately before subcutaneous implantation or subsequent to the tube being placed in the femoral defect.

### 2.4. BMP-2 Release from Alginate Constructs

Release of BMP-2 from alginate constructs into 0.1% (w/v) BSA in PBS was monitored over 21 days at 37°C. Alginate constructs were fabricated with or without 1 mg of HMPs

and 2.5 μg of BMP-2. HMPs were loaded with BMP-2 in a small volume of 0.1% BSA in 4 mM HCl (25 μL/mg HMPs) for 16 hours at 4°C the day before construct assembly. BMP-2 was added either directly into the alginate solution or loaded onto the MPs and then added into the alginate solution. Constructs were transferred to individual wells of an ultra-low attachment 24-well plate (Corning) and 1 mL of 0.1% BSA in PBS was added. At various time points over 21 days, the solution was completely removed and replaced with fresh 0.1% BSA in PBS. Release samples were analyzed for BMP-2 content via enzyme linked immunosorbent assay (ELISA; R&D Systems, Minneapolis, MN).

### 2.5. Fluorescent Labeling of BMP-2 and Heparin Microparticles

BMP-2 was fluorescently labeled using Vivotag-S 750 Flurochrome (VS750; Perkin Elmer, Waltham, MA; Ex: 750 nm, Em: 780 nm), which contains an amine reactive NHS ester. 100 μg/mL of BMP-2 in 100 mM $NaH_2PO_4$ (pH = 7.4) (Sigma Aldrich) was combined with a 10-fold molar excess of VS750 label, and the reaction proceeded at room temperature in the dark for 4 hours. The solution was dialyzed against 100 mM $NaPO_4$ using a Slide-A-Lyzer MINI dialysis device (volume ratio = 1:70, molecular weight cut off = 3.5 kDa; Thermo Fisher Scientific) for 16 hours to remove hydrolyzed NHS and unreacted label. BMP-2 labeling and removal of excess dye was confirmed by gel electrophoresis, followed by near infrared imaging on an Odyssey gel scanner (Li-cor Biotechnology, Lincoln, NE). BMP-2 was stored at −20°C until use.

Fluorescently labeled HMPs were fabricated by conjugation of Alexa Fluor 647 hydrazide (AF647; Thermo Fisher Scientific; Ex: 650 nm, Em: 670 nm) to heparin methacrylamide prior to HMP formation. 0.6 mM heparin methacrylamide was reconstituted in 100 mM $NaPO_4$ (pH = 7.4) and combined with 0.1 M 1-ethyl-3-(3-dimethylaminopropyl) carbodiimide hydrochloride (EDC) and 1 mM AF647 hydrazide; the reaction proceeded at room temperature in the dark for 2 hours. The reaction volume was dialyzed against water (volume ratio = 1:40, molecular weight cut off = 3.5 kDa; Spectrum Laboratories) for 24 hours, lyophilized, and stored at 4°C until use.

### 2.6. Subcutaneous Implant Surgical Procedure

Subcutaneous implant studies were performed to (1) determine the persistence of HMPs within the alginate constructs, (2) evaluate the ability of constructs with or without BMP-2 and HMPs to form ectopic mineral, and (3) track retention of BMP-2 in constructs with or without HMPs. All surgical procedures were conducted according to Georgia Institute of Technology Institutional Animal Care and Use Committee (IACUC) protocols. 13-week-old female Sprague Dawley rats (Charles River Labs, Wilmington, MA) were anesthetized using isoflurane. Two lateral incisions were made on the back of each animal and a tunneling device was used to create four individual subcutaneous pockets for construct insertion, as previously described [33]. A metal rod and cannula were used to insert two constructs near the forelimbs and two near the hind limbs. Placement of constructs from each group was distributed between the four locations.

For HMP retention and ectopic mineralization studies, constructs consisted of PCL meshes containing (1) 150 μL alginate (n=6), (2) 1 mg of labeled HMPs in 150 μL alginate (n=6),

(3) 5 μg of BMP-2 in 150 μL alginate (n=6), and (4) 5 μg of BMP-2 loaded onto 1 mg of labeled HMPs in 150 μL alginate (n=6). Animals for these studies were euthanized after 6 weeks. For BMP-2 tracking studies, constructs consisted of PCL meshes containing (1) 2.5 μg of labeled BMP-2 in 150 μL alginate (n=3) and (2) 2.5 μg of labeled BMP-2 loaded onto 1 mg of HMPs in 150 μL alginate (n=3). These animals were euthanized after 3 weeks.

### 2.7. Fluorescence Imaging

Fluorescent imaging was performed with an IVIS® Spectrum instrument (Perkin Elmer). For evaluation of AF647-labeled HMP retention, constructs were imaged *ex vivo* (Ex: 640, Em: 720) prior to subcutaneous implantation and immediately after explanting at 6 weeks. Constructs were placed on glass slides for imaging as depicted and oriented such that the same number of perforations were visible in each mesh tube (Figure 3A). For VS750-labeled BMP-2 tracking, longitudinal *in vivo* imaging (Ex: 745, Em: 800) was performed on Day 0, 4, 7, 10, and 14. Animals were placed on their sides for imaging two constructs at once. Total fluorescent counts and radiant efficiency (p/sec•sr•μW) were evaluated for each construct at each time point, using a ~7 $cm^2$ elliptical region of interest (ROI) in Living Image Software (Perkin Elmer). Background fluorescence from the skin was evaluated for each animal in an ROI away from the implanted constructs and subtracted from each measurement. Fluorescent signal at each time point was normalized to the initial fluorescent signal measured *in vivo* at Day 0.

### 2.8. Femoral Defect Surgical Procedure

Femoral defect studies were undertaken to determine the ability of constructs with and without HMPs and BMP-2 to promote bone healing in a critically sized defect. 13-week-old female Sprague Dawley rats were anesthetized using isoflurane prior to surgery, and bilateral segmental defect surgeries were performed as previously described [18, 36]. A radiolucent polysulfone fixation plate and two stainless steel risers were screwed directly onto the femur for limb stabilization, and an oscillating saw was used to create an 8-mm wide, full thickness defect. A PCL mesh tube was inserted into the defect to cover the bone ends, and 150 μL of alginate was injected through the perforations into the center of the tube. Alginate hydrogels contained one of the following: (1) 1 mg of unloaded HMPs (n =4), (2) 2.5 μg of BMP-2 (n=5), or (3) 2.5 μg of BMP-2 loaded onto 1 mg of HMPs (n=5). These treatment groups were distributed among animals such that similar numbers of each were implanted in the left and right femurs. Animals for these studies were euthanized using carbon dioxide asphyxiation at 2 or 12 weeks post-surgery.

### 2.9. Radiography and Micro-Computed Tomography

Subcutaneously implanted constructs were harvested after 6 weeks, and mineralization was evaluated. *Ex vivo* micro-computed tomography (CT) was performed (microCT42 scanner, Scanco, Switzerland) using a voxel size of 16 μm, voltage of 55 kVp, and current of 145 μA [37, 38]. A threshold of 80 was set for new mineral formation, and a Gaussian filter (sigma = 1.2, support = 1) was applied to suppress noise. Longitudinal *in vivo* radiographs of femurs were obtained at 2, 4, 8, and 12 weeks post-surgery, using a Faxitron MX-20 Digital machine at a voltage of 23 kV and exposure time of 15 seconds. Radiographs were used to qualitatively assess bony bridging across the defect. *In vivo* micro-CT of femurs was

performed at 4, 8, and 12 weeks post-surgery using a VivaCT40 live animal scanner (Scanco) at medium resolution, with a voxel size of 38.5 μm, voltage of 55 kVp, and current of 109 μA [19]. Mineral was quantified within the central 6 mm region (160 scan slices) of each 8 mm defect, to avoid artifacts caused by the appearance of the metal risers on the CT scans. A global threshold for new bone formation was set at 50% of the average mineral density of native cortical bone, and noise was suppressed using a Gaussian filter (sigma = 1.2, support = 1).

### 2.10. Biomechanical Testing

Femurs removed from rats at 12 weeks underwent mechanical testing using a uniaxial torsion testing system (Bose EnduraTEC ELF200; Bose Electroforce Systems Group, Eden Prairie, MN). The strength of the regenerated bone in the defect was compared to that of native bone (age-matched historical data). Briefly, fixation plates and soft tissue were removed from isolated femora, before the bone ends were placed in molten Wood's metal (Alfa Aesar, Haverhill, MA), allowed to solidify, and mounted into the machine. Torsion was applied at a rate of 3º per second until failure, allowing for the determination of maximum torque and calculation of torsional stiffness, using the slope of the linear segment of the torque-rotation curve.

### 2.11. Histological Sectioning and Staining

To determine the distribution of HMPs within alginate hydrogels, constructs with or without 1 mg of HMPs (n=3) were fabricated and processed for cryosectioning. Constructs were incubated in successively more concentrated solutions of sucrose and optimal cutting temperature (OCT) compound (Sakura Finetek USA Inc., Torrance, CA) at room temperature under vacuum to promote complete infiltration of OCT compound into the hydrogel matrix. Constructs were then transferred to 100% OCT compound and frozen in a bath of 100% ethanol and dry ice. 5 μm cryo-sections were stained with Safranin O to visualize alginate and HMPs.

For subcutaneous implant studies, all constructs were collected for histology at 6 weeks post-surgery. For femoral defect studies, femurs from each treatment group exhibiting representative bone formation were isolated for histology at 2 and 12 weeks post-surgery. After harvesting, the constructs and femurs were fixed in 10% neutral buffered formalin at 4°C for 24 and 48 hours, respectively, followed by decalcification at room temperature using a formic acid decalcifier (Cal Ex-II, Thermo Fisher Scientific) with gentle agitation and replacement of the solution every 2–3 days for 2 weeks. Complete decalcification of constructs and femurs was verified radiographically. Samples were dehydrated through submersion in a series of alcohol and xylene solutions and vacuum-embedded in paraffin wax (Paraplast, Sigma Aldrich) at 60°C.

5 μm midsagittal sections of the defects were cut for histological analysis. Safranin O/Fast Green staining was performed to characterize HMP and alginate persistence, mineral formation, and gross tissue morphology. Immunohistochemistry for Ki-67 antigen was performed using a mouse MIB-5 antibody (1:50, Dako, Carpinteria, CA), followed by a horseradish peroxidase (HRP) conjugated secondary antibody (Vector Labs, Burlingame,

CA) and 3,3'diaminobenzidine (DAB) staining, to evaluate cell proliferation within the bone defect. Gill's hematoxylin was used to visualize cell nuclei, and Safranin O was used to visualize HMPs. Histological sections of rat small intestine served as a Ki-67 positive control (Figure S2B). Separate sections were treated with non-immune mouse serum (Invitrogen), followed by the horseradish peroxidase secondary antibody, as a control for non-specific antibody binding (Figure S2A).

### 2.12. COMSOL Model Development

COMSOL Multiphysics software (Version 5.2a; Burlington, MA) was used to develop a computational model to describe BMP-2 release from alginate constructs *in vivo*. Diffusion profiles of BMP-2 in the construct and surrounding tissues were simulated with and without HMPs to determine the role of BMP-2-HMP interactions in BMP-2 release. The 3D geometries of the cylindrical alginate construct and thigh were reduced to a 2D axisymmetric modeling domain consisting of two nested rectangles. The reaction engineering physics module was coupled with the transport of dilute species physics module to model BMP-2 interactions with HMPs and BMP-2 diffusion through alginate hydrogel and surrounding tissue. Equations for BMP-2 interactions with HMPs, BMP-2 diffusion through alginate, and BMP-2 diffusion through tissue were based on Fick's laws of diffusion and simple binding kinetics described by Crank [39]. The change in BMP-2 concentration in the alginate hydrogel over time was described as

$$\frac{\partial c_{BMP,Alg}}{\partial t} = \nabla \cdot \left(\mathrm{D}_{BMP,Alg} \nabla c_{BMP,Alg}\right) + R_{BMP,Alg} \quad \text{(Eqn. 1)}$$

in which $D_{BMP,Alg}$ = diffusion coefficient of BMP-2 through alginate ($cm^2/s$), $C_{BMP,Alg}$ = BMP-2 concentration in alginate ($mol/m^3$), and $R_{BMP,Alg}$ = rate of BMP-2 appearance/disappearance through HMP association/dissociation. Similarly, the change in BMP-2 concentration in the thigh tissue over time was defined by

$$\frac{\partial c_{BMP,Tiss}}{\partial t} = \nabla \cdot \left(\mathrm{D}_{BMP,Tiss} \nabla c_{BMP,Tiss}\right) \quad \text{(Eqn. 2)}$$

in which $D_{BMP,Tiss}$ = diffusion coefficient of BMP-2 through tissue ($cm^2/s$) and $C_{BMP,Tiss}$ = BMP-2 concentration in tissue ($mol/m^3$). Finally, the rate of BMP-2 appearance/disappearance in the alginate hydrogel due to association/dissociation from HMPs was described as

$$R_{BMP,Alg} = k_{off} C_{BMP+MP} - k_{on} C_{BMP} C_{MP} \quad \text{(Eqn. 3)}$$

in which $C_{BMP+MP}$ = bound HMP-BMP-2 complexes ($mol/m^3$), $C_{BMP}$ = free BMP-2 ($mol/m^3$), and $C_{MP}$ = empty HMP binding sites ($mol/m^3$). The association and dissociation rate constants to BMP-2 binding to HMPs were $k_{on}$ ($1/nM \cdot s$) and $k_{off}$ ($1/s$), respectively.

It was assumed that, over the timeframe simulated (14 days), the alginate hydrogel did not appreciably degrade, based on the comparison between initial *in vitro* histology images and *in vivo* histology images after 2 weeks, as well as previous data [21]. Thus $D_{BMP,Alg}$ was not time-dependent, and HMPs did not move or leave the construct boundary ($D_{BMP+MP,Alg}$ = $D_{MP,Alg}$ = 0). Alginate and thigh tissue were modeled as liquids in an unmixed batch reactor to allow spatially constrained transport of BMP-2. Additionally, to further simplify the complex *in vivo* environment such that simulations could be performed, interstitial fluid flow was considered negligible in comparison to the diffusivities of BMP-2 through the construct and tissue.

The necessary parameters were defined (Table 1) to compute solutions for constructs containing 2.5 μg of BMP-2 delivered within alginate or loaded onto 0.1 or 1 mg of HMPs. The effective diffusion coefficient of BMP-2 through alginate ($D_{BMP,Alg}$) was calculated based on experimental data collected from *in vitro* diffusion experiments, while the effective diffusion coefficient of BMP-2 through the surrounding mesh tube and thigh tissue ($D_{BMP,Tiss}$) was approximated using previous BMP-2 retention data obtained through fluorescent BMP-2 tracking in the segmental bone defect [18]. The number of BMP-2 binding sites on HMPs was calculated on a per molecule basis using a previously established maximum binding capacity of HMPs (~300 μg BMP-2/mg HMPs) [32]. Data on the release of BMP-2 from HMPs in serum was used to establish association and dissociation rate constants chosen that accurately described BMP-2-HMP interactions. Rate constants were initially chosen based on literature values for BMP-2 binding to linear heparin ($K_D$ = 20 nM, $k_{on}$ = 5.1e-04 1/nM•s, $k_{off}$ = 0.01 1/s) [40] and subsequently adjusted for HMPs using a COMSOL model of *in vitro* BMP-2-HMP interactions in serum [41], which revealed that a higher dissociation rate constant than that of linear heparin was necessary to accurately model the experimental results ($K_D$ = 500 nM, $k_{on}$ = 5.1e-04 1/nM•s, $k_{off}$ = 0.25 1/s). Finally, $D_{BMP,Alg}$, $D_{BMP,Tiss}$, and $K_D$ were varied by +/−10% to evaluate the sensitivity of the model to changes in these key parameters.

### 2.13. Statistical Analysis

All data are reported as mean ± standard deviation. *In vitro* experiments were performed with a minimum of 3 replicates for each experimental group, and 3–6 constructs per group were implanted for subcutaneous implant experiments. Segmental defect surgeries were performed on 4–5 femurs per group, such that longitudinal micro-CT was conducted on 4–5 femurs per group and biomechanical testing was conducted on 3–4 femurs per group. Normality of the data was assessed using the Shapiro-Wilk test. Statistical significance was determined using one-way or two-way ANOVA as appropriate, followed by Bonferroni's post hoc analysis (Graphpad Prism, Version 5.0, La Jolla, CA). For data that did not satisfy the assumptions of equal variances and Gaussian distributions (Figures 3C and 5C), the nonparametric Kruskal-Wallis test was used. $p < 0.05$ was considered statistically significant.

# 3. Results

## 3.1. Bioactivity of Microparticle-Bound BMP-2

We have previously demonstrated that HMPs can bind BMP-2 and maintain protein bioactivity over short periods of time *in vitro* (3 days), to induce ALP activity in C2C12 myoblasts [32]. Since other studies have demonstrated that heparin can extend BMP-2 bioactivity *in vitro* [42, 43], we evaluated whether loading HMPs with BMP-2 would result in a similar effect on long-term BMP-2 bioactivity. Representative images of C2C12 cells after 3 days with (Figure 1E) and without (Figure 1D) DMMB-stained HMPs depict typical cell and MP coverage using 0.1 mg of HMPs in a 96-well plate. BMP-2-loaded HMPs induced higher total ALP activity than unloaded HMPs and soluble BMP-2 when used immediately (0 weeks) and after 2 weeks of pre-incubation in cell culture media (Figure 1B). While the ALP activity induced by BMP-2-loaded HMPs and soluble BMP-2 dropped significantly over 2 weeks, there was no difference between the ALP activity induced by pre-incubated loaded HMPs at 2 weeks and newly reconstituted soluble BMP-2, indicating that HMPs could maintain BMP-2 bioactivity at a similar level to fresh protein, even after 2 weeks of incubation in serum-containing media. Moreover, unlike soluble BMP-2, BMP-2-loaded HMPs increased the DNA content of cultures regardless of pre-incubation (Figure 1C), similar to our previous results [32]. When ALP activity was normalized to DNA content, soluble BMP-2 and BMP-2-loaded HMPs induced similar ALP activity with or without pre-incubation (Figure S1).

## 3.2. In Vitro Characterization of Alginate Constructs

In Safranin O stained cryo-sections of alginate constructs, HMPs appeared as dark red, punctate circles, while alginate stained lighter orange-red (Figure 2A). HMPs (indicated by black arrows) were well distributed throughout the alginate. The volume of 1 mg of HMPs comprised <4% of the volume of the hydrogel, and did not appear to visibly impact hydrogel formation. All BMP-2-containing constructs demonstrated slow, gradual BMP-2 release over 21 days. Constructs containing BMP-2 entrapped directly within the alginate exhibited higher total BMP-2 release at later time points (Day 14 and 21, $p < 0.01$) compared to constructs containing BMP-2 loaded onto HMPs (Figure 2B).

## 3.3. Subcutaneous Implantation of Alginate Constructs

*Ex vivo* fluorescence imaging of alginate constructs containing Alexa Fluor 647-labeled HMPs (unloaded or BMP-2-loaded) revealed persistence of approximately 55% of the original fluorescent signal after 6 weeks of subcutaneous implantation (Figure 3B). There were no differences in fluorescence retention between unloaded HMPs (HMP) and BMP-2-loaded HMPs (HMP + BMP-2). Micro-CT quantification of ectopic mineralization in subcutaneously implanted constructs demonstrated low mineral volume in constructs containing alginate only and unloaded HMPs after 6 weeks. Constructs containing BMP-2 entrapped in alginate and BMP-2 loaded HMPs demonstrated variable amounts of mineralized tissue formation (Figure 3C). Due to the inconsistency in mineral formation caused by animal-to-animal variability and variability in construct placement, among other factors, there were no differences in average mineral volumes of any of the groups ($p = 0.07$ between BMP-2 and alginate alone and $p = 0.09$ between HMP + BMP-2 and alginate

alone). Safranin O/Fast Green staining of constructs revealed mineral in both BMP-2 and BMP-2-loaded HMP constructs (blue/green staining indicated by white arrows; Figure 3D, E), while constructs containing unloaded HMPs were primarily filled with fibrous tissue (Figure 3F). Safranin O staining also depicted residual alginate (orange/red staining) in all groups and the persistence of intact HMPs in all HMP-containing constructs (intense red staining of discrete round shapes indicated yellow arrows). Alginate constructs containing fluorescently labeled BMP-2 were implanted subcutaneously to track *in vivo* BMP-2 retention over time. Representative IVIS® images and quantification of fluorescent signal normalized to Day 0 values revealed decreasing fluorescent signal in all constructs over time (Figure 4A–E). BMP-2 retention in constructs with HMPs was transiently greater than constructs without HMPs at Days 4 and 7 (Figure 4E).

### 3.4. Orthotopic Mineralization in Femoral Defects

Femoral defects were treated with alginate containing BMP-2, BMP-2-loaded HMPs, or unloaded HMPs. After 12 weeks, mineralized bridging (i.e. continuous bone throughout the defect) was observed in all defects treated with BMP-2 (5/5), 60% of defects treated with BMP-2-loaded HMPs (MP + BMP-2) (3/5), and none of the defects treated with unloaded HMPs (0/4). Representative radiographs illustrate the progression of bone formation in defects over time (Figure 5A). Of defects treated with loaded HMPs, three bridged completely (top row), while two exhibited bone formation throughout the defect but did not bridge (bottom row). Longitudinal *in vivo* micro-CT scans revealed minimal bone formation in defects treated with unloaded HMPs, and higher bone volumes in both BMP-2-containing groups (Figure 5B). Overall, BMP-2-loaded HMPs induced less mineral formation than BMP-2 alone ($p < 0.001$); however, these differences were not significant at individual time points. Additionally, no differences in mineral density of bone regenerate were observed between femurs treated with BMP-2 and loaded HMPs (data not shown). Femurs underwent torsion testing after 12 weeks post-surgery (Figure 5C); both bridged and non-bridged samples from BMP-2-treated groups were tested. No differences in maximum torque were observed between femurs treated with BMP-2 and loaded HMPs, nor were the maximum torques different from that of intact femurs.

### 3.5. Histological Analysis of Femoral Defects

Safranin O/Fast Green stained sections of 12-week femurs revealed residual alginate (shown in red) in all groups. Bone formation was evident in femurs treated with BMP-2 and loaded HMPs (blue/green staining indicated by white arrows; Figure 6A, C). Femurs treated with unloaded HMPs did not display any appreciable bone formation, and only fibrous tissue was observed, interspersed between alginate and remaining HMPs (red staining of discrete round shapes indicated by yellow arrows; Figure 6B). Femurs treated with BMP-2-loaded HMPs demonstrated similar bone morphology to femurs treated with BMP-2 delivered in the alginate, with mineral in close proximity to residual alginate and intact HMPs (Figure 6C).

Immunolocalization of the cell proliferation marker Ki-67 was performed on femurs obtained 2 weeks post-surgery, to allow adequate time for cellular infiltration and yet ensure persistence of BMP-2 within the constructs. Immunohistochemistry revealed minimal Ki-67$^{+}$ staining in femurs treated with BMP-2 alone (Figure 6D). However, femurs treated

with unloaded HMPs and BMP-2-loaded HMPs exhibited Ki-67$^+$ cell nuclei throughout the defect, with some co-localized cells and HMPs (Figure 6E, F), suggesting that cells infiltrating the defect site were proliferating in response to HMPs but not in response to BMP-2 entrapped in alginate.

### 3.6. COMSOL Modeling of In Vivo BMP-2 Diffusion

Given that the presence of HMPs within alginate constructs transiently increased BMP-2 retention in the defect and increased the amount of bone formation, COMSOL Multiphysics Software was used to model BMP-2 release from constructs into the surrounding tissue, in an attempt to explain the results observed *in vivo*. Simulations revealed drastically different BMP-2 release profiles between 2.5 μg of BMP-2 delivered in alginate and 2.5 μg of BMP-2 loaded onto 1 mg of HMPs (Figure 7). When BMP-2 was delivered in the alginate hydrogel (Figure 7A, B), 86% of the BMP-2 was predicted to be released from the construct over 14 days. Conversely, when the same amount of BMP-2 was delivered using HMPs (Figure 7C, D), the model predicted that only 2.8% of the BMP-2 delivered was released into the surrounding tissue and 0.8% was released within the alginate, while ~97% of the delivered BMP-2 remained immobilized by the HMPs. Interestingly, when simulations were run using a lower dose of HMPs (0.1 mg), the model predicted an increase in BMP-2 release into the surrounding tissue (16%) and alginate (6%), with only ~77% of the delivered BMP-2 remaining associated with the HMPs. A sensitivity analysis of several key parameters ($D_{BMP,\ Alg}$, $D_{BMP,\ Tiss}$, and $K_D$) revealed low sensitivity to +/−10% changes (Table S1). Overall BMP-2 released into the tissue changed from 2.8% of BMP-2 delivered to 2.5–3.1%, which does not represent a biologically significant change in this model. Thus, we did not expect discrepancies in the values assigned to these parameters to significantly alter the results obtained.

## 4. Discussion

Heparin, with its known affinity for binding many potent growth factors, has been incorporated into biomaterial delivery vehicles to prolong the local persistence of biomolecules. For example, the covalent conjugation of heparin on PLGA scaffolds extended the time for total BMP-2 release from less than four hours to three weeks [44], while the incorporation of 1–10% heparin into hyaluronan microgels dose-dependently increased BMP-2 loading and decreased BMP-2 release [45]. In this study, we investigated the addition of HMPs into alginate constructs as a facile means of altering the spatial distribution of BMP-2 *in vivo*. We demonstrated that HMPs, which comprised <4% of the volume of the construct, could be evenly dispersed throughout alginate by simple mixing without any indication of disrupting hydrogel formation. Loading BMP-2 onto HMPs prolonged BMP-2 bioactivity and reduced *in vitro* BMP-2 release from alginate constructs by ~45% compared to constructs containing BMP-2 alone. Moreover, HMPs were retained within constructs implanted subcutaneously and in femoral bone defects, where the HMPs increased early BMP-2 retention and supported bone formation.

Few studies have investigated the effects of heparin modification of biomaterials on *in vivo* growth factor retention, due, in part, to the challenge of consistently and accurately

retrieving or detecting proteins implanted within deeper tissues, which can mask biomaterial-related differences in protein retention. To investigate BMP-2 release *in vivo*, we took advantage of fluorescence imaging techniques, which have been previously used to track PDGF-BB and BMP-2 in bone defects for 2–3 weeks post-surgery [17, 18, 46]. We implanted alginate constructs in superficial locations along the dorsal surface of rats, to maximize the sensitivity of *in vivo* fluorescence detection. While the ideal environment to investigate BMP-2 release would be directly within bone defects, in which many different cell types and biomolecules reside, significant technical obstacles limit image-based detection of fluorescent molecules implanted deeper within tissues [34]. Additionally, previous studies have reported consistent BMP-2 release profiles from subcutaneous and bone defect sites [47], despite stark differences in the extent of vasculature between the two locations. Constructs containing BMP-2-loaded HMPs increased BMP-2 retention at early time points, yet resulted in similar BMP-2 retention to constructs containing BMP-2 delivered from the hydrogel after 2 weeks. BMP-2 release was also notably higher *in vivo* than *in vitro*, which may be attributed to fluorophore degradation, differences in detection methods (colorimetric ELISA substrate *in vitro* vs. fluorescence *in vivo*), hydrogel leaking out of the construct into the subcutaneous environment, and the presence of numerous proteases, cells, and heparin-binding proteins that could accelerate BMP-2 release and degradation. We have previously demonstrated that heparin-binding serum proteins can displace BMP-2 bound to HMPs and increase BMP-2 release *in vitro* [41]; thus, competitive binding of blood-borne proteins to HMPs *in vivo* may similarly displace BMP-2 and decrease its retention in implanted constructs.

Despite similar BMP-2 retention after 14 days *in vivo*, constructs containing BMP-2-loaded HMPs induced bony bridging of only 60% of treated femoral defects, and the volume of bone regenerated was only ~75% of that when BMP-2 was delivered from the alginate alone. Since we previously demonstrated that HMPs can effectively present bioactive BMP-2 to induce cellular responses upon contact [32], and that HMPs can maintain long-term BMP-2 bioactivity, these data suggest that increased BMP-2 retention by HMPs at early time points (4 and 7 days) may have resulted in a suboptimal initial release and spatial gradient of BMP-2 from the construct, subsequently decreasing chemotaxis and early cell infiltration into the alginate hydrogel [7, 48]. In our previous work, we highlighted the importance of BMP-2 presentation, demonstrating that barriers to cell-HMP contact, such as transwell separation, decreased the efficiency of C2C12 ALP induction [32]. Inadequate cell infiltration may have similarly reduced the ability of cells to interact with HMP-bound BMP-2. Furthermore, the dosing of BMP-2 and HMPs in this study resulted in a theoretical concentration of ~5 million BMP-2 molecules per HMP. Since HMPs are of a similar size as cells and are expected to retain the majority of loaded BMP-2, the high density of heparin within HMPs may have resulted in focal concentrations of BMP-2 and less uniform presentation to cells compared to the more homogenous, diffuse distribution of BMP-2 anticipated with hydrogel delivery. On the other hand, loaded HMPs within implanted constructs may have also provided a prolonged BMP-2 stimulus to infiltrating cells. We demonstrated that loading HMPs with BMP-2 *in vitro* better preserves long term BMP-2 bioactivity compared to soluble BMP-2, similar to the protective effect of linear heparin on growth factor activity [42, 43].

A computational model was developed to further investigate the effect of HMPs on *in vivo* BMP-2 release kinetics, in a manner that would otherwise be experimentally challenging. *In silico* models describing *in vitro* growth factor release have been created to optimize delivery vehicles containing various affinity molecules [49–51]. Interestingly, our model predicted that the addition of 1 mg of HMPs in the alginate construct would almost completely abrogate BMP-2 release *in vivo*, reducing total BMP-2 release from 86% to 2.8%. This low release of BMP-2 was predicted due to the large excess of BMP-2 binding sites (~6.9E15) available within constructs containing 1 mg of HMPs, which could increase re-association of BMP-2 that had previously dissociated from HMPs. Although attenuated BMP-2 release may explain the reduced healing response observed following HMP-mediated BMP-2 delivery, the loss of BMP-2 fluorescence and robust bone formation makes it unlikely that only 3% of delivered BMP-2 entered the surrounding tissue. This discrepancy between *in vivo* experimental data and *in silico* model simulations may be due to biological factors that could not be accurately recapitulated in this model, including early alginate degradation, changes in material diffusivity following cell infiltration and healing, and substantial interstitial fluid flow. Despite these shortcomings, the COMSOL model provides insight into the role of HMP-BMP-2 interactions in the generation of a BMP-2 spatial gradient *in vivo*. Simulations run using a lower dose of HMPs (0.1 mg) for BMP-2 delivery predicted that decreasing the number of available binding sites for BMP-2 could increase BMP-2 release into the surrounding tissue from 2.8% to 16%, while maintaining a high local concentration of BMP-2 within the femoral defect (77%). Furthermore, *in vitro* BMP-2 release experiments conducted in serum instead of PBS yielded association and dissociation rate constants more suitable to modeling the *in vivo* environment. When included in an adjusted simulation, these parameters could yield a more predicative and useful model of BMP-2 release, which could be used to tune HMP-BMP-2 interactions *in silico* prior to *in vivo* investigation.

Finally, in addition to the role HMPs played in altering BMP-2 release from constructs, we found that HMP persistence *in vivo* also influenced cell proliferation. In ectopic and orthotopic sites, HMPs persisted within the constructs for at least 6 and 12 weeks post-surgery, respectively. Both unloaded and BMP-2-loaded HMPs had the additional effect of inducing early cell proliferation in the bone defect, as evidenced by Ki-67$^{+}$ staining in HMP-treated defects after 2 weeks post-surgery. We previously observed enhanced C2C12 proliferation in the presence of BMP-2-loaded HMPs *in vitro* [32], speculating that persistent BMP-2 signaling or presentation of other mitogenic proteins on HMPS may have induced a proliferative response. Similar events may be occurring in the bone defect, and the competitive binding of serum borne, heparin-binding proteins may further modulate cell proliferation *in vivo* [52–54].

## 5. Conclusions

*In vivo* delivery of BMP-2 using HMPs incorporated in hydrogel constructs increased BMP-2 retention and cell proliferation within implantation sites and induced robust mineral formation in femoral defects. Interestingly, despite increased BMP-2 retention *in vivo*, HMP-mediated delivery of BMP-2 decreased bone formation in comparison to delivery of BMP-2 in alginate alone. These results demonstrate that increasing BMP-2 retention within

the site of bone injury does not necessarily result in improved bone formation and thus should not be the only goal of biomaterial delivery strategies. Since the addition of HMPs into the hydrogel constructs did not completely abrogate bone formation, our results further suggest that BMP-2 presentation within the defect and BMP-2 release into the surrounding tissues may both play important roles in facilitating bone regeneration. Finally, the *in silico* model predictions of BMP-2 release suggest that changing the number of HMPs delivered to the bone defect may provide a convenient method of tuning *in vivo* BMP-2 retention and release. Thus, with the help of computational modeling tools and further *in vivo* investigation, HMPs could be optimized to facilitate a suitable ratio of BMP-2 retention and release and have the potential to serve as a valuable BMP-2 delivery vehicle in the future.

## Supplementary Material

Refer to Web version on PubMed Central for supplementary material.

## Acknowledgements

The authors acknowledge Ashley Allen, Brett Klosterhoff, David Reece, Marissa Ruehle, Giuliana Salazar-Noratto, Sanjay Sridaran, and Brennan Torstrick for their assistance with surgeries. BMP-2 was provided by Pfizer Inc. This work was supported by funding from the National Institutes of Health (R01 AR062006 to TCM) and the Armed Forces Institute of Regenerative Medicine (Award W81XWH-14-2-0003 to REG). The U.S. Army Medical Research Acquisition Activity is the awarding and administering acquisition office. Opinions, interpretations, conclusions, and recommendations are those of the authors and are not necessarily endorsed by the Department of Defense. MHH was supported by a Natural Sciences and Engineering Research Council of Canada (NSERC) post-graduate scholarship and Philanthropic Educational Organization (PEO) Scholar Award. CC was supported by the Petit Undergraduate Research Scholars Program at Georgia Tech.

## 7. References

[1]. Blank E, Lappan C, Belmont PJ Jr, Shaun Machen M, Ficke J, Pope R, Owens BD, Early analysis of the United States Army's telemedicine orthopaedic consultation program, J Surg Orthop Adv 20(1) (2011) 50. [PubMed: 21477534]

[2]. Laurencin C, Khan Y, El-Amin SF, Bone graft substitutes, (2006).

[3]. Kolar P, Schmidt-Bleek K, Schell H, Gaber T, Toben D, Schmidmaier G, Perka C, Buttgereit F, Duda GN, The early fracture hematoma and its potential role in fracture healing, Tissue Eng Part B 16(4) (2010) 427–434.

[4]. Einhorn TA, Clinical Applications of Recombinant Human BMPs: Early Experience and Future Development, The Journal of Bone & Joint Surgery 85(suppl_3) (2003) 82–88. [PubMed: 12925614]

[5]. Urist MR, Mikulski A, Lietze A, Solubilized and insolubilized bone morphogenetic protein, Proc Natl Acad Sci USA 76(4) (1979) 1828–1832. [PubMed: 221908]

[6]. Wozney JM, Rosen V, Celeste AJ, Mitsock LM, Whitters MJ, Kriz RW, Hewick RM, Wang EA, Novel Regulators of Bone Formation: Molecular Clones and Activities, Science 242(4885) (1988) 1528–1534. [PubMed: 3201241]

[7]. Uludag H, D'Augusta D, Palmer R, Timony G, Wozney J, Characterization of rhBMP-2 pharmacokinetics implanted with biomaterial carriers in the rat ectopic model, J Biomed Mater Res 46(2) (1999) 193–202. [PubMed: 10379997]

[8]. Uludag H, D'Augusta D, Golden J, Li J, Timony G, Riedel R, Wozney JM, Implantation of recombinant human bone morphogenetic proteins with biomaterial carriers: a correlation between protein pharmacokinetics and osteoinduction in the rat ectopic model, J Biomed Mater Res 50(2) (2000) 227–238. [PubMed: 10679688]

[9]. Uludag H, Friess W, Williams D, Porter T, Timony G, D'Augusta D, Blake C, Palmer R, Biron B, Wozney J, rhBMP-Collagen Sponges as Osteoinductive Devices: Effects of in Vitro Sponge

Characteristics and Protein pI on in Vivo rhBMP Pharmacokinetics, Ann N Y Acad Sci 875(1) (1999) 369–378. [PubMed: 10415583]

[10]. Smucker JD, Rhee JM, Singh K, Yoon ST, Heller JG, Increased swelling complications associated with off-label usage of rhBMP-2 in the anterior cervical spine, Spine 31(24) (2006) 2813–9. [PubMed: 17108835]

[11]. Shields LB, Raque GH, Glassman SD, Campbell M, Vitaz T, Harpring J, Shields CB, Adverse effects associated with high-dose recombinant human bone morphogenetic protein-2 use in anterior cervical spine fusion, Spine 31(5) (2006) 542–547. [PubMed: 16508549]

[12]. Wong DA, Kumar A, Jatana S, Ghiselli G, Wong K, Neurologic impairment from ectopic bone in the lumbar canal: a potential complication of off-label PLIF/TLIF use of bone morphogenetic protein-2 (BMP-2), Spine J 8(6) (2008) 1011–1018. [PubMed: 18037352]

[13]. Woo EJ, Adverse events after recombinant human BMP2 in nonspinal orthopaedic procedures, Clinical Orthopaedics and Related Research® 471(5) (2013) 1707–1711. [PubMed: 23132207]

[14]. Boraiah S, Paul O, Hawkes D, Wickham M, Lorich DG, Complications of recombinant human BMP-2 for treating complex tibial plateau fractures: a preliminary report, Clinical Orthopaedics and Related Research® 467(12) (2009) 3257–3262. [PubMed: 19693635]

[15]. Lutolf MP, Weber FE, Schmoekel HG, Schense JC, Kohler T, Müller R, Hubbell JA, Repair of bone defects using synthetic mimetics of collagenous extracellular matrices, Nature biotechnology 21(5) (2003) 513–518.

[16]. Jeon O, Powell C, Solorio LD, Krebs MD, Alsberg E, Affinity-based growth factor delivery using biodegradable, photocrosslinked heparin-alginate hydrogels, Journal of Controlled Release 154(3) (2011) 258–266. [PubMed: 21745508]

[17]. Shekaran A, García JR, Clark AY, Kavanaugh TE, Lin AS, Guldberg RE, García AJ, Bone Regeneration using an Alpha 2 Beta 1 Integrin-Specific Hydrogel as a BMP-2 Delivery Vehicle, Biomaterials 35(21) (2014) 5453–5461. [PubMed: 24726536]

[18]. Boerckel JD, Kolambkar YM, Dupont KM, Uhrig BA, Phelps EA, Stevens HY, García AJ, Guldberg RE, Effects of protein dose and delivery system on BMP-mediated bone regeneration, Biomaterials 32(22) (2011) 5241–5251. [PubMed: 21507479]

[19]. Kolambkar YM, Dupont KM, Boerckel JD, Huebsch N, Mooney DJ, Hutmacher DW, Guldberg RE, An alginate-based hybrid system for growth factor delivery in the functional repair of large bone defects, Biomaterials 32(1) (2011) 65–74. [PubMed: 20864165]

[20]. Priddy LB, Chaudhuri O, Stevens HY, Krishnan L, Uhrig BA, Willett NJ, Guldberg RE, Oxidized alginate hydrogels for bone morphogenetic protein-2 delivery in long bone defects, Acta Biomater 10(10) (2014) 4390–4399. [PubMed: 24954001]

[21]. Krishnan L, Priddy LB, Esancy C, Klosterhoff BS, Stevens HY, Tran L, Guldberg RE, Delivery vehicle effects on bone regeneration and heterotopic ossification induced by high dose BMP-2, Acta Biomater 49 (2017) 101–112. [PubMed: 27940197]

[22]. Mehta M, Schmidt-Bleek K, Duda GN, Mooney DJ, Biomaterial delivery of morphogens to mimic the natural healing cascade in bone, Adv Drug Deliv Rev 64(12) (2012) 1257–1276. [PubMed: 22626978]

[23]. Pakulska MM, Miersch S, Shoichet MS, Designer protein delivery: From natural to engineered affinity-controlled release systems, Science 351(6279) (2016) aac4750. [PubMed: 26989257]

[24]. Hettiaratchi M, Guldberg R, McDevitt T, Biomaterial strategies for controlling stem cell fate via morphogen sequestration, J Mater Chem B (2016).

[25]. Miller T, Goude MC, McDevitt TC, Temenoff JS, Molecular engineering of glycosaminoglycan chemistry for biomolecule delivery, Acta Biomater 10(4) (2014) 1705–1719. [PubMed: 24121191]

[26]. Jeon O, Song SJ, Kang S-W, Putnam AJ, Kim B-S, Enhancement of ectopic bone formation by bone morphogenetic protein-2 released from a heparin-conjugated poly (L-lactic-co-glycolic acid) scaffold, Biomaterials 28(17) (2007) 2763–2771. [PubMed: 17350678]

[27]. Kim SE, Song S-H, Yun YP, Choi B-J, Kwon IK, Bae MS, Moon H-J, Kwon Y-D, The effect of immobilization of heparin and bone morphogenic protein-2 (BMP-2) to titanium surfaces on inflammation and osteoblast function, Biomaterials 32(2) (2011) 366–373. [PubMed: 20880582]

[28]. Hannink G, Geutjes PJ, Daamen WF, Buma P, Evaluation of collagen/heparin coated TCP/HA granules for long-term delivery of BMP-2, Journal of Materials Science: Materials in Medicine 24(2) (2013) 325–332. [PubMed: 23135410]

[29]. Johnson MR, Boerckel JD, Dupont KM, Guldberg RE, Functional restoration of critically sized segmental defects with bone morphogenetic protein-2 and heparin treatment, Clin Orthop Relat Res 469(11) (2011) 3111–3117. [PubMed: 21863396]

[30]. Park K-H, Kim H, Moon S, Na K, Bone morphogenic protein-2 (BMP-2) loaded nanoparticles mixed with human mesenchymal stem cell in fibrin hydrogel for bone tissue engineering, Journal of Bioscience and Bioengineering 108(6) (2009) 530–537. [PubMed: 19914589]

[31]. He T, Wu D, Wang X, Rong J, Zhao J, Photo-crosslinking hyaluronan-heparin hybrid hydrogels for BMP-2 sustained delivery, Journal of Polymer Engineering (2016).

[32]. Hettiaratchi MH, Miller T, Temenoff JS, Guldberg RE, McDevitt TC, Heparin microparticle effects on presentation and bioactivity of bone morphogenetic protein-2, Biomaterials 35(25) (2014) 7228–7238. [PubMed: 24881028]

[33]. Allen AB, Gazit Z, Su S, Stevens HY, Guldberg RE, In vivo bioluminescent tracking of mesenchymal stem cells within large hydrogel constructs, Tissue Engineering Part C: Methods 20(10) (2014) 806–816. [PubMed: 24576050]

[34]. Troy T, Jekic-McMullen D, Sambucetti L, Rice B, Quantitative comparison of the sensitivity of detection of fluorescent and bioluminescent reporters in animal models, Mol Imaging 3(1) (2004) 9–23. [PubMed: 15142408]

[35]. Einhorn TA, Clinically applied models of bone regeneration in tissue engineering research, Clin Orthop Relat Res 367 (1999) S59–S67.

[36]. Oest ME, Dupont KM, Kong HJ, Mooney DJ, Guldberg RE, Quantitative assessment of scaffold and growth factor-mediated repair of critically sized bone defects, Journal of orthopaedic research 25(7) (2007) 941–950. [PubMed: 17415756]

[37]. Dosier CR, Uhrig BA, Willett NJ, Krishnan L, Li M-TA, Stevens HY, Schwartz Z, Boyan BD, Guldberg RE, Effect of cell origin and timing of delivery for stem cell-based bone tissue engineering using biologically functionalized hydrogels, Tissue Engineering Part A 21(1–2) (2014) 156–165. [PubMed: 25010532]

[38]. Freeman FE, Allen AB, Stevens HY, Guldberg RE, McNamara LM, Effects of in vitro endochondral priming and pre-vascularisation of human MSC cellular aggregates in vivo, Stem cell research & therapy 6(1) (2015) 1. [PubMed: 25559585]

[39]. Crank J, The mathematics of diffusion, Oxford university press1979.

[40]. Ruppert R, Hoffmann E, Sebald W, Human bone morphogenetic protein 2 contains a heparin-binding site which modifies its biological activity, Eur J Biochem 237(1) (1996) 295–302. [PubMed: 8620887]

[41]. Hettiaratchi MH, Chou C, Servies N, Smeekens JM, Cheng A, Esancy C, Wu R, McDevitt T, Guldberg R, Krishnan LN, Competitive protein binding influences heparin-based modulation of spatial growth factor delivery for bone regeneration, Tissue Eng Part A (ja) (2017).

[42]. Zhao B, Katagiri T, Toyoda H, Takada T, Yanai T, Fukuda T, Chung U.-i., Koike T, Takaoka K, Kamijo R, Heparin potentiates the in vivo ectopic bone formation induced by bone morphogenetic protein-2, J Biol Chem 281(32) (2006) 23246–23253. [PubMed: 16754660]

[43]. Bhakta G, Rai B, Lim ZX, Hui JH, Stein GS, van Wijnen AJ, Nurcombe V, Prestwich GD, Cool SM, Hyaluronic acid-based hydrogels functionalized with heparin that support controlled release of bioactive BMP-2, Biomaterials 33(26) (2012) 6113–6122. [PubMed: 22687758]

[44]. Jeon O, Song SJ, Kang S-W, Putnam AJ, Kim B-S, Enhancement of ectopic bone formation by bone morphogenetic protein-2 released from a heparin-conjugated poly (l-lactic-*co*-glycolic acid) scaffold, Biomaterials 28(17) (2007) 2763–2771. [PubMed: 17350678]

[45]. Zhao J, Luo C, Chen Y, Wu D, Shen C, Han W, Tu M, Zeng R, Preparation, structure and BMP-2 controlled release of heparin-conjugated hyaluronan microgels, Carbohyd Polym 86(2) (2011) 806–811.

[46]. Shah NJ, Hyder MN, Quadir MA, Courchesne N-MD, Seeherman HJ, Nevins M, Spector M, Hammond PT, Adaptive growth factor delivery from a polyelectrolyte coating promotes

synergistic bone tissue repair and reconstruction, Proceedings of the National Academy of Sciences 111(35) (2014) 12847–12852.

[47]. Kempen DH, Lu L, Heijink A, Hefferan TE, Creemers LB, Maran A, Yaszemski MJ, Dhert WJ, Effect of local sequential VEGF and BMP-2 delivery on ectopic and orthotopic bone regeneration, Biomaterials 30(14) (2009) 2816–2825. [PubMed: 19232714]

[48]. Lind M, Eriksen E, Bünger C, Bone morphogenetic protein-2 but not bone morphogenetic protein-4 and-6 stimulates chemotactic migration of human osteoblasts, human marrow osteoblasts, and U2-OS cells, Bone 18(1) (1996) 53–57. [PubMed: 8717537]

[49]. Sakiyama-Elbert SE, Hubbell JA, Development of fibrin derivatives for controlled release of heparin-binding growth factors, J Control Release 65(3) (2000) 389–402. [PubMed: 10699297]

[50]. Wood MD, Sakiyama-Elbert SE, Release rate controls biological activity of nerve growth factor released from fibrin matrices containing affinity-based delivery systems, J Biomed Mater Res 84A(2) (2008) 300–312.

[51]. Vulic K, Pakulska MM, Sonthalia R, Ramachandran A, Shoichet MS, Mathematical model accurately predicts protein release from an affinity-based delivery system, J Control Release 197 (2015) 69–77. [PubMed: 25449806]

[52]. Majack RA, Goodman LV, Dixit VM, Cell surface thrombospondin is functionally essential for vascular smooth muscle cell proliferation, The Journal of cell biology 106(2) (1988) 415–422. [PubMed: 2448314]

[53]. García AJ, Vega M.a.D., Boettiger D, Modulation of cell proliferation and differentiation through substrate-dependent changes in fibronectin conformation, Molecular biology of the cell 10(3) (1999) 785–798. [PubMed: 10069818]

[54]. Swertfeger DK, Hui DY, Apolipoprotein E Receptor Binding VersusHeparan Sulfate Proteoglycan Binding in Its Regulation of Smooth Muscle Cell Migration and Proliferation, Journal of Biological Chemistry 276(27) (2001) 25043–25048. [PubMed: 11350966]

## Statement of Significance

The development of effective biomaterials for sustained protein delivery is a crucial component of tissue engineering strategies. However, in most applications, including bone repair, the optimal balance between protein presentation in the injury site and protein release into the surrounding tissues is unknown. Herein, we introduced heparin microparticles (HMPs) into a tissue engineered construct to increase *in vivo* retention of bone morphogenetic protein-2 (BMP-2) and enhance healing in femoral defects. Although HMPs induced bone regeneration, no increase in bone volume was observed, leading to further experimental and computational analysis of the effect of HMP-BMP-2 interactions on protein retention and release. Ultimately, this work provides insight into designing tunable protein-material interactions and their implications for controlling BMP-2 delivery.

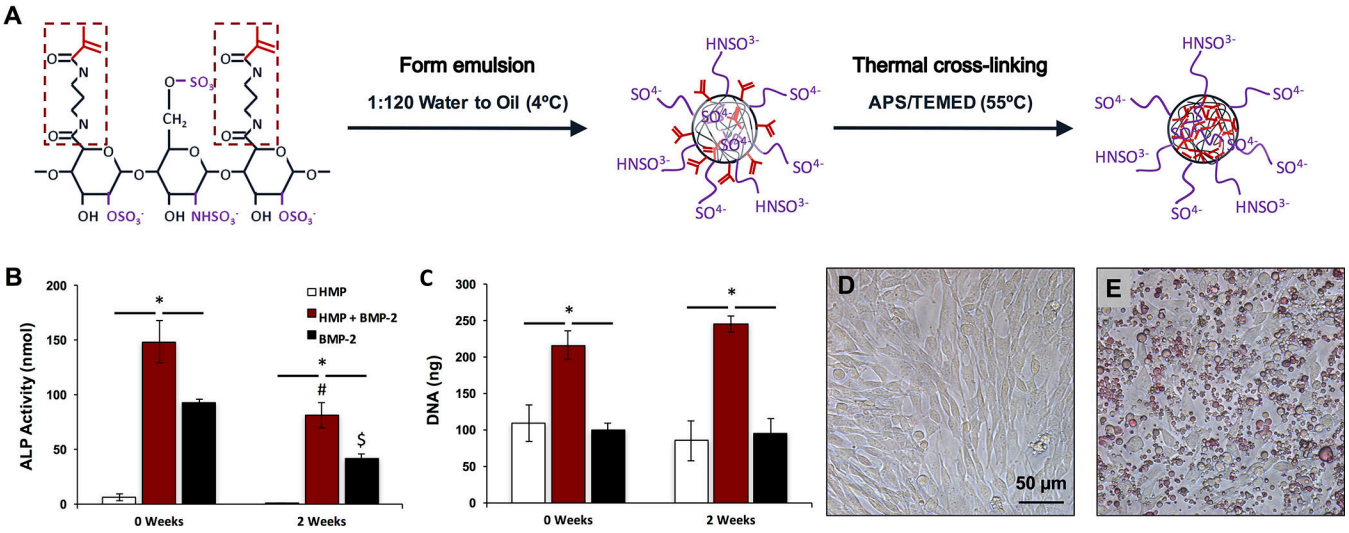


**Figure 1.**

Heparin microparticle fabrication and in vitro characterization. A) Schematic of HMP fabrication process. Heparin methacrylamide was dissolved in water and emulsified in oil. The emulsion was heated to promote free radial cross-linking of the methacrylamide groups. B) HMP-bound BMP-2 bioactivity was evaluated by culturing C2C12 cells for 72 h with soluble BMP-2 and BMP-2-loaded HMPs, and evaluating ALP activity and DNA content. BMP-2-loaded HMPs induced higher total ALP activity than unloaded HMPs or soluble BMP-2, but ALP activity induced by both BMP-2-containing groups decreased after 2 weeks of pre-incubation at 37 ºC. (* = $p < 0.05$ as indicated; # = $p < 0.05$ compared to loaded MPs (0 weeks); $ = $p < 0.05$ compared to soluble BMP-2 (0 weeks)) C) BMP-2-loaded HMPs yielded greater DNA content after 3 days compared to unloaded HMPs and soluble BMP-2 treatment at both 0 and 2 weeks. (* = $p < 0.05$ as indicated) D) Representative images of C2C12 cells cultured for 72 h alone or E) with 0.1 mg of HMPs stained with DMMB for contrast.

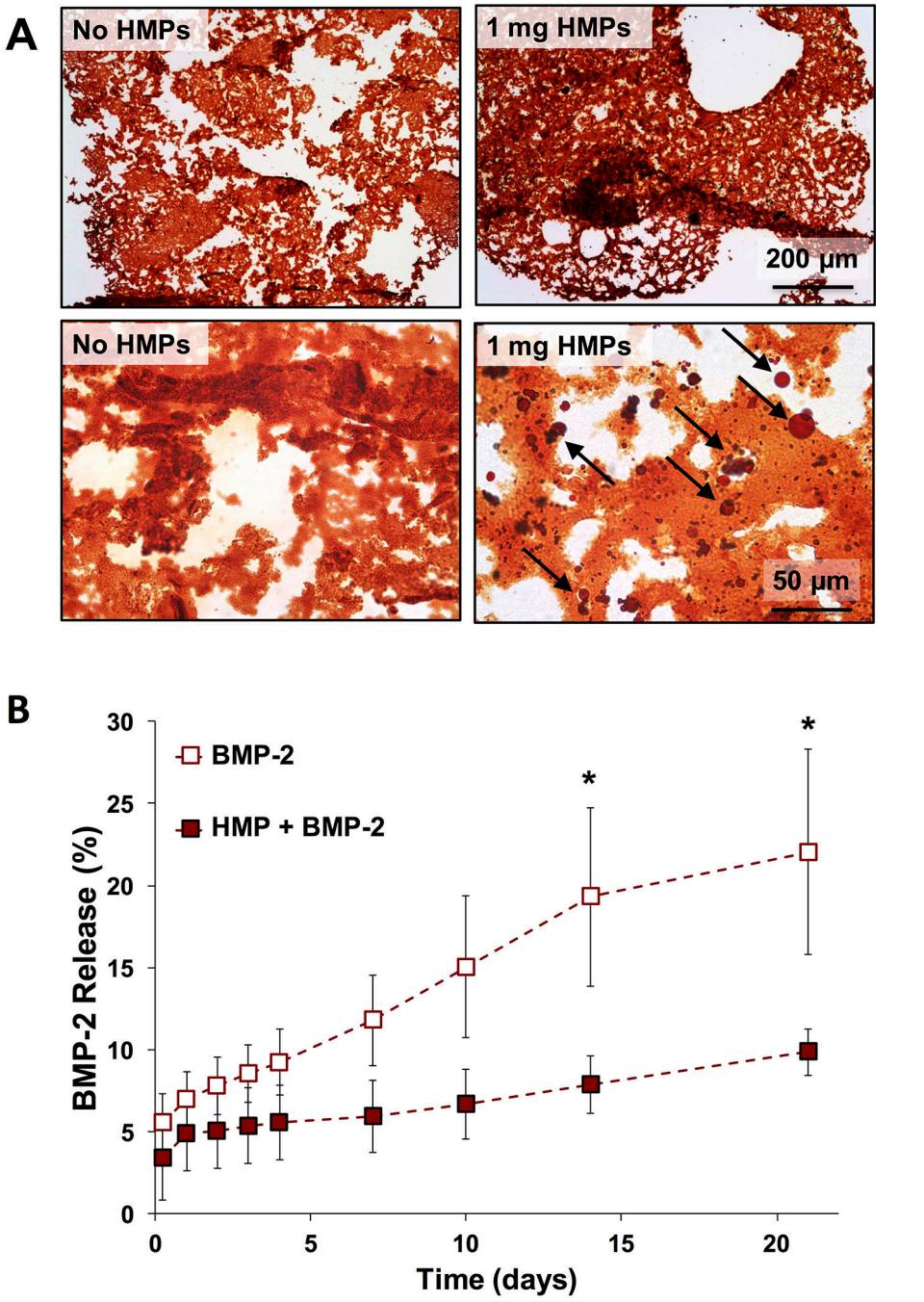


**Figure 2.**

In vitro characterization of alginate tissue engineered constructs. A) Representative images of Safranin O-stained sections of alginate constructs without HMPs or containing 1 mg of HMPs. Black arrows indicate HMPs. B) BMP-2 release was evaluated from alginate constructs containing 2.5 μg of soluble BMP-2 or BMP-2 loaded onto 1 mg of HMPs. Cumulative BMP-2 release from constructs without HMPs was greater than BMP-2 release from HMP-containing constructs after 2 and 3 weeks. (* = $p < 0.05$ between groups at indicated time points).

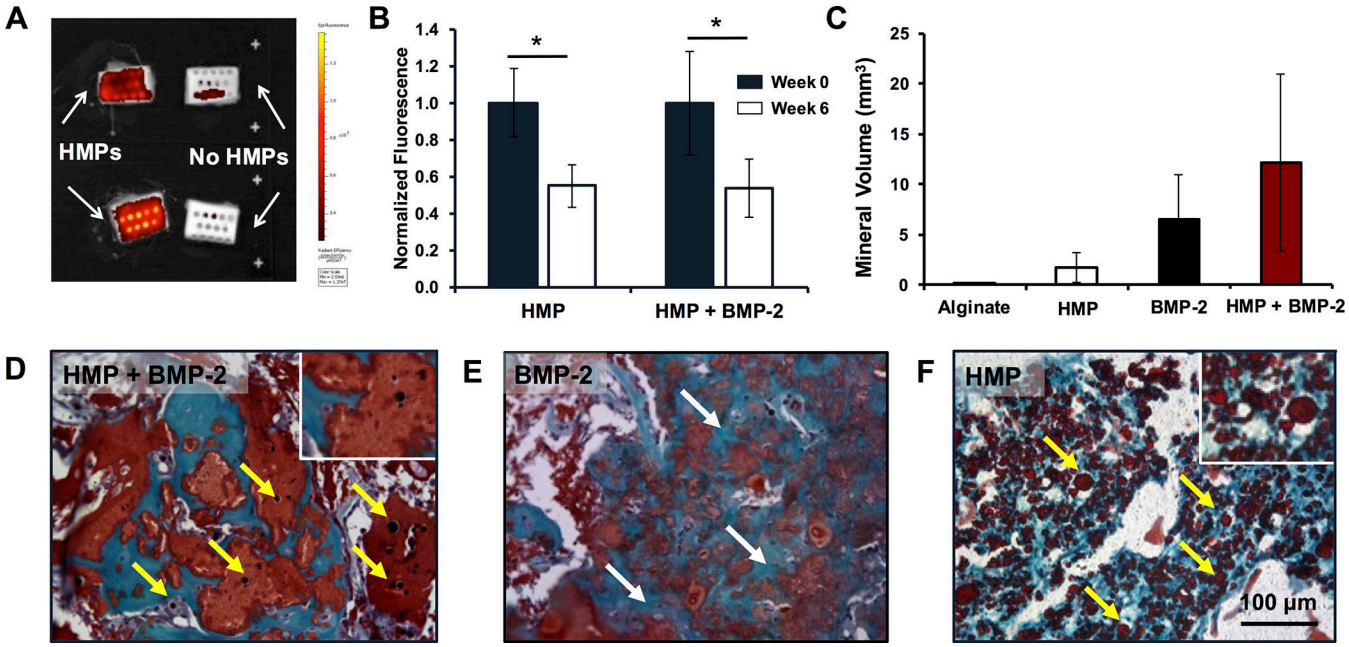


**Figure 3.**

Ectopic mineralization and retention of heparin microparticles in subcutaneously implanted alginate constructs. 1 mg of AF647-labeled HMPs (unloaded or loaded with 5 μg of BMP-2) were mixed into alginate constructs, which were implanted subcutaneously in the backs of rats for 6 weeks (n = 6). A) Representative IVIS® image (Ex: 640, Em: 720) depicting explanted constructs with and without labeled HMPs after 6 weeks. B) Fluorescent signal of constructs, normalized to initial fluorescence, immediately prior to implantation (Week 0) and following explanting (Week 6). AF647 signal decreased over time in both unloaded and loaded HMP-containing constructs. (* = $p < 0.05$ as indicated) C) Micro-CT quantification of mineral volume induced in constructs. No differences were observed between groups. Safranin O/Fast Green staining of alginate constructs containing D) BMP-2-loaded HMPs, E) BMP-2 only, and F) unloaded HMPs depicted mineralization (white arrows) in BMP-2-containing constructs and the presence of intact HMPs (yellow arrows) in HMPs-containing constructs after 6 weeks in vivo.

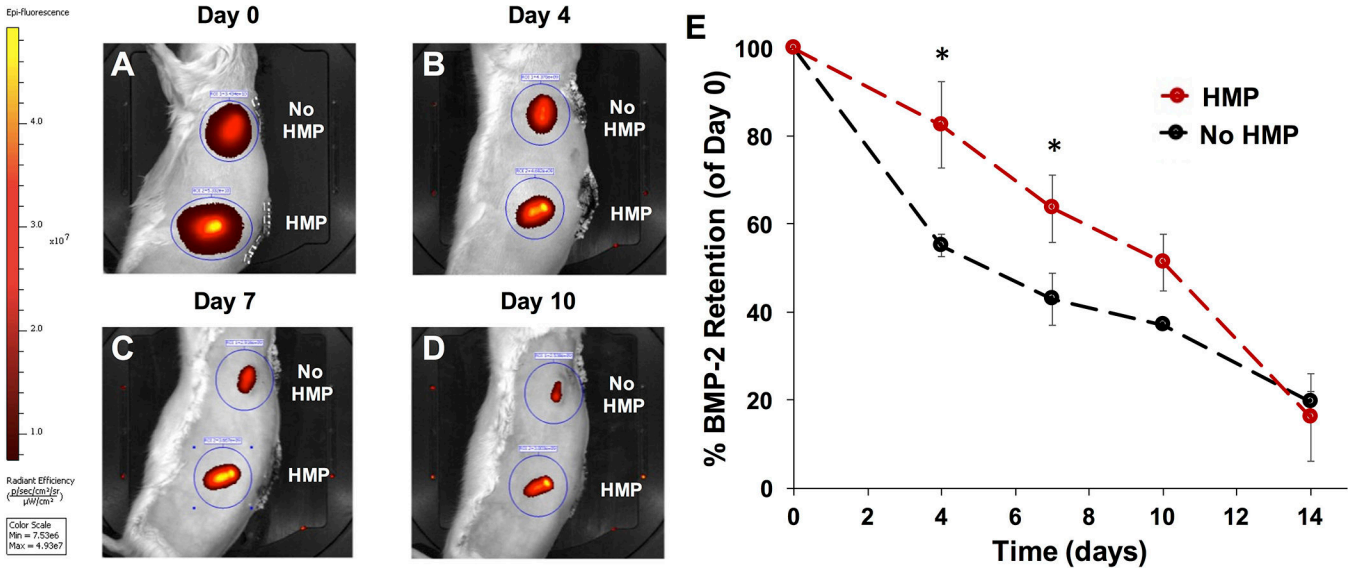


**Figure 4.**

Longitudinal BMP-2 tracking within subcutaneously implanted alginate constructs. VS750-labeled BMP-2 (2.5 μg alone or loaded onto 1 mg of HMPs) were mixed into 150 μL of 2% RGD-alginate. Alginate constructs were implanted subcutaneously in the backs of rats for 3 weeks (n = 3) and imaged on an IVIS® platform at 0, 4, 7, 10, and 14 days after surgery. A–D) Representative fluorescence IVIS® images of subcutaneous implants at indicated time points. E) Quantification of in vivo VS750 fluorescence in implantation sites (normalized to Day 0 fluorescence) demonstrated increased fluorescence in HMP-containing groups at 4 and 7 days post-surgery. (* = $p < 0.05$ as indicated).

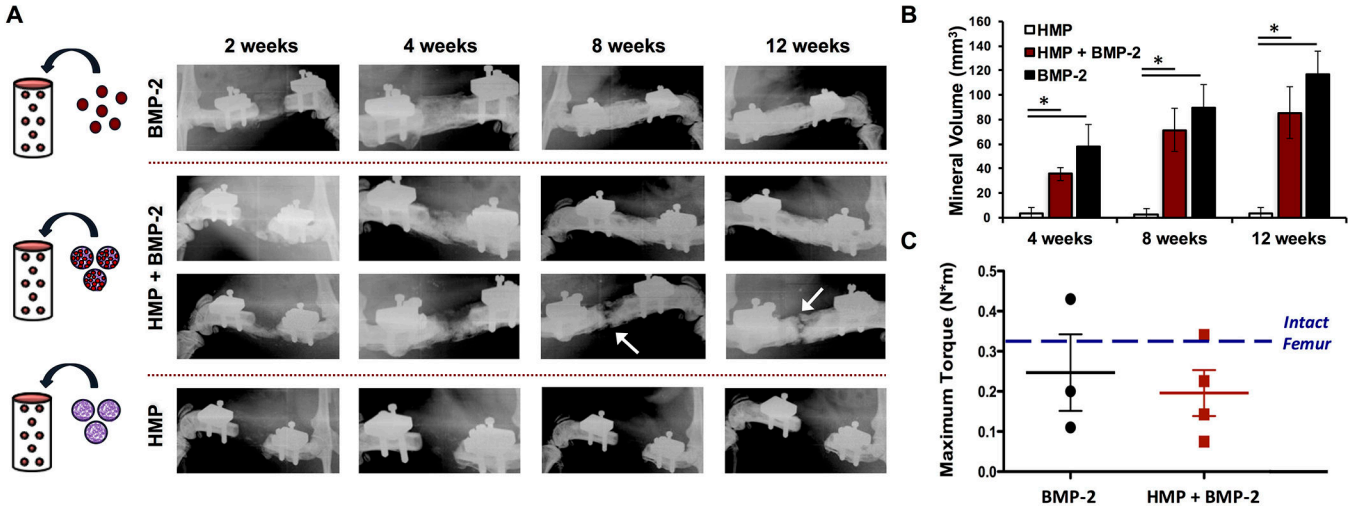


**Figure 5.**

Assessment of orthotopic mineralization in femoral defects treated with alginate constructs. A) Femoral defects were treated with alginate constructs containing 1 mg of unloaded HMPs, 1 mg of HMPs loaded with 2.5 μg of BMP-2, or 2.5 μg of BMP-2 (n = 4–5). Representative radiographs of femurs at 2, 4, 8, and 12 weeks post-surgery. All of the defects treated with BMP-2 alone bridged (5/5), whereas only some of the defects containing HMP + BMP-2 bridged (3/5), and no defects containing unloaded HMPs bridged. Radiographs of femurs treated with BMP-2-loaded HMPs are representative of both bridging and non-bridging cases. White arrows indicate gaps in mineral formation in non-bridged defects. B) Micro-CT quantification of mineral volume in bone defects at 4, 8, and 12 weeks post-surgery. Both BMP-2 and BMP-2-loaded HMP treated femurs demonstrated greater bone formation than unloaded HMPs at each time point (* = $p < 0.05$ as indicated). BMP-2 treatment induced more bone formation than loaded HMPs overall ($p < 0.001$). C) Explanted femurs underwent torsion to failure after 12 weeks post-surgery (n = 3–4). No differences in maximum torque were observed between the BMP-2 treated groups or compared to intact femurs of age-matched rats (historical data [16]).

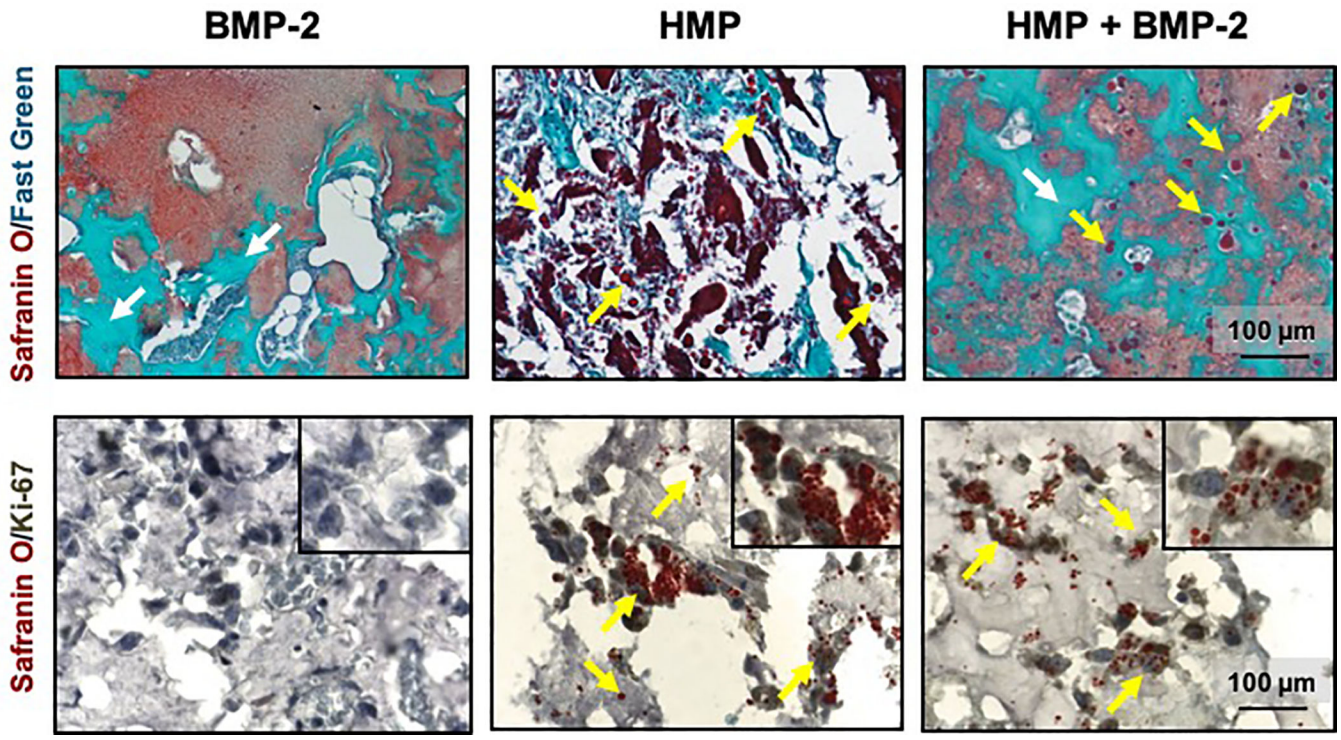


**Figure 6.**

Histological analysis of regenerated femurs. Safranin O/Fast Green staining of representative femurs treated for 12 weeks with A) 2.5 lg of BMP-2, B) 1 mg of unloaded HMPs, and C) 2.5 μg of BMP-2 loaded onto 1 mg of HMPs. Ki67 antibody staining of femurs treated for 2 weeks with D) 2.5 μg of BMP-2, E) 1 mg of unloaded HMPs, and F) 2.5 μg of BMP-2 loaded onto 1 mg of HMPs. Yellow arrows indicate HMPs, and white arrows indicate new bone formation. (For interpretation of the references to colour in this figure legend, the reader is referred to the web version of this article.)

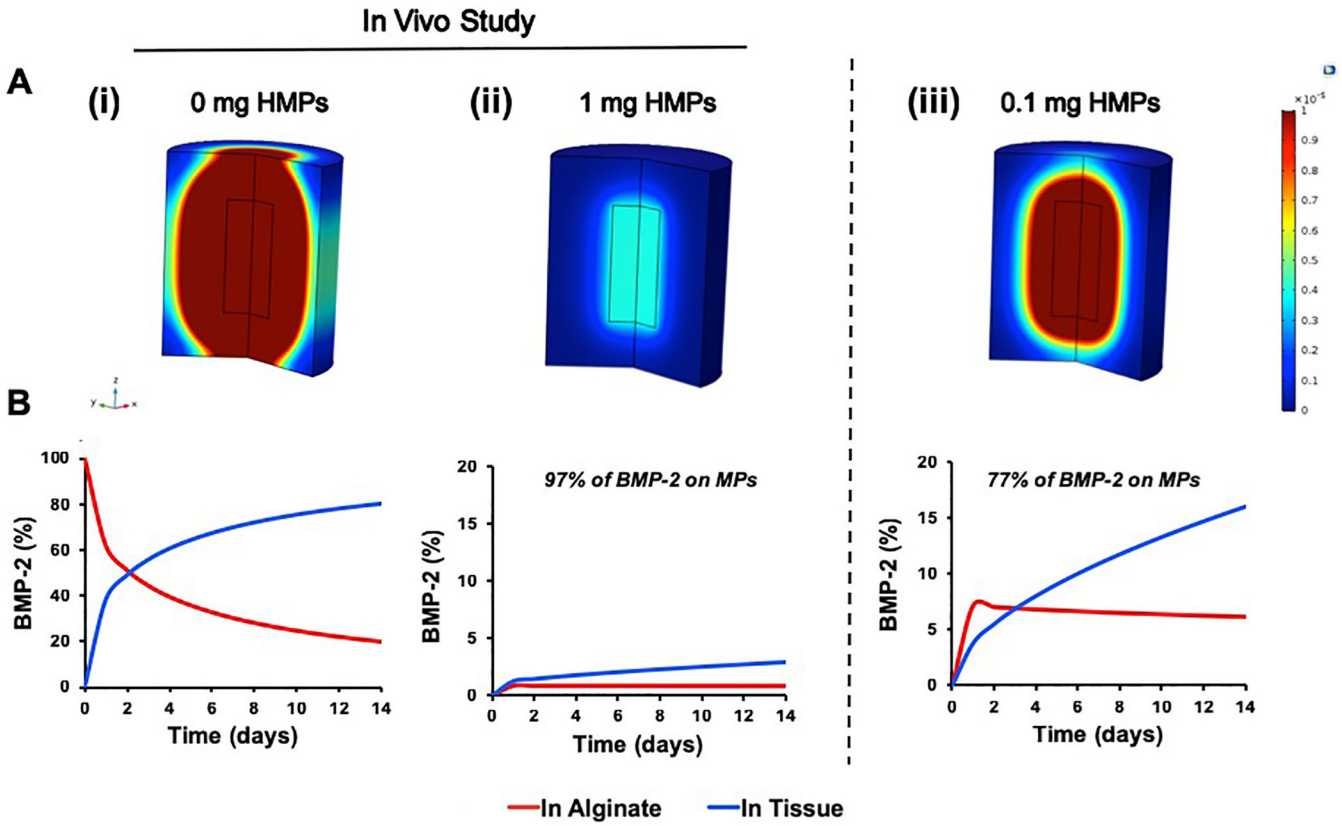


**Figure 7.**

COMSOL simulations of BMP-2 release from alginate constructs in femoral defects. BMP-2 release simulations of constructs containing 2.5 μg of BMP-2 in alginate, BMP-2 loaded onto 1 mg of HMPs in alginate, and BMP-2 loaded onto 0.1 mg of HMPs in alginate. Constructs without HMPs and with 1 mg of HMPs were tested in vivo. A) Heat maps after 14 days demonstrated (i) a large spatial gradient of BMP-2 in femurs treated with BMP-2 in alginate, (ii) a minimal spatial gradient of BMP-2 in femurs treated with BMP-2 loaded onto 1 mg of HMPs in alginate, and (iii) a moderate spatial gradient of BMP-2 in femurs treated with BMP-2 loaded onto 0.1 mg of HMPs in alginate. Similarly, graphs of the simulation results revealed (i) an increase the percentage of BMP-2 released into the surrounding tissue and decrease in the percentage of BMP-2 remaining within the alginate in constructs containing BMP-2 alone, (ii) most of the delivered BMP-2 remaining bound to the HMPs over 14 days in constructs containing 1 mg of HMPs, and (iii) a moderate release of BMP-2 into the surrounding tissue and high retention of BMP-2 in the alginate in constructs containing 0.1 mg of HMPs.

**Table 1.**

Parameters Used in COMSOL Model of BMP-2 Release in Femoral Defect

| Category | Parameter | Value | Reference |
|---|---|---|---|
| **Dimensions** | Diameter of Alginate Cylinder | 4.5 mm | |
| | Length of Alginate Cylinder | 10 mm | |
| | Diameter of Thigh Cylinder | 15 mm | |
| | Length of Thigh Cylinder | 18 mm | |
| **BMP-2 Diffusion Through Alginate** | Effective Diffusion Coefficient ($D_{BMP,Alg}$) | 1.7E-06 $cm^2/s$ | |
| **BMP-2 Diffusion Through Thigh** | Effective Diffusion Coefficient ($D_{BMP,Tiss}$) | 2.0E-08 $cm^2/s$ | [18] |
| **BMP-2 Interactions with HMPs** | Weight of HMPs | 0.1 mg, 1 mg | |
| | Number of HMPs | 2.0E06, 2.0E07 | |
| | Number of Binding Sites | 7.0E14, 7.0E15 | |
| | Number of BMP-2 Molecules | 5.8E13 | |
| | Dissociation Constant ($K_D$) | 50 nM | Adapted from [40] |
| | Dissociation Rate Constant ($k_{on}$) | 5.1E-04 1/nM•s | Adapted from [40] |
| | Association Rate Constant ($k_{off}$) | 0.25 1/s | Adapted from [40] |